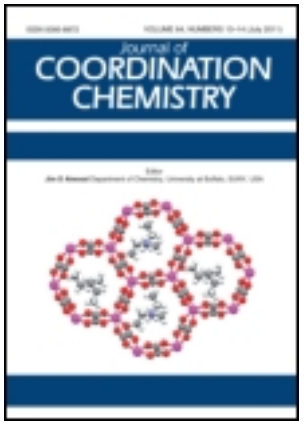

Journal of Coordination Chemistry
Publication details, including instructions for authors and subscription information:
http://www.tandfonline.com/loi/gcoo20

π-π Stacking and magnetic coupling mechanism on a mononuclear Cu(II) complex

Hong Li [a], Shi-Guo Zhang [a], Long-Miao Xie [b], Li Yu [b] & Jing-Min Shi [b]

[a] Binzhou Key Laboratory of Material Chemistry, Department of Chemistry and Chemical Engineering, Binzhou University, Binzhou 256603, P.R. China

[b] Department of Chemistry, Shandong Normal University, Jinan 250014, P.R. China

Published online: 21 Oct 2011.

To cite this article: Hong Li, Shi-Guo Zhang, Long-Miao Xie, Li Yu & Jing-Min Shi (2011) π-π Stacking and magnetic coupling mechanism on a mononuclear Cu(II) complex, Journal of Coordination Chemistry, 64:20, 3595-3608, DOI: 10.1080/00958972.2011.625019

To link to this article: http://dx.doi.org/10.1080/00958972.2011.625019

Journal of Coordination Chemistry
Vol. 64, No. 20, 20 October 2011, 3595–3608

$\pi-\pi$ Stacking and magnetic coupling mechanism on a mononuclear Cu(II) complex

HONG LI†, SHI-GUO ZHANG†, LONG-MIAO XIE‡, LI YU‡ and JING-MIN SHI*‡

†Binzhou Key Laboratory of Material Chemistry, Department of Chemistry and Chemical Engineering, Binzhou University, Binzhou 256603, P.R. China
‡Department of Chemistry, Shandong Normal University, Jinan 250014, P.R. China

(*Received 15 April 2011; in final form 31 August 2011*)

A mononuclear copper(II) complex was synthesized and in the crystal there are three types of $\pi-\pi$ stacking interactions among adjacent complexes. The fitting for the data of the variable-temperature magnetic susceptibilities reveals that there is a weak anti-ferromagnetic coupling among adjacent Cu(II) ions with Weiss constant $\theta=-2.99$ K $=-2.08\,cm^{-1}$. Theoretical calculations reveal that two types of $\pi-\pi$ stacking resulted in anti-ferromagnetic couplings with $2J=-12.40\,cm^{-1}$ and $2J=-9.74\,cm^{-1}$, respectively, and the third type of $\pi-\pi$ stacking led to a weak ferromagnetic interaction with $2J=4.28\,cm^{-1}$. The theoretical calculations also indicate that the ferromagnetic coupling sign from the $\pi-\pi$ stacking accords with McConnell I spin-polarization mechanism, whereas the anti-ferromagnetic coupling signs cannot be explained with McConnell I spin-polarization mechanism.

Keywords: Crystal structure; Magnetic coupling; $\pi-\pi$ Stacking; Copper complex; Theoretical calculation; Broken-symmetry theory

1. Introduction

Molecular magnetism has attracted attention and major advances have been made in description and application as new molecular-based materials [1–3]. In reported molecular magnetic compounds absolute majority spin carriers, such as metallic ions and radicals, deal with systems where the coupling spin carriers are connected by bridging ligands [4–8]; the magnetic interactions are through bond exchange whereas $\pi-\pi$ stacking interaction has also been playing a pivotal role in the magnetic interaction. For example, some authors attributed strong ferromagnetic order to $\pi-\pi$ stacking interaction [9], and other authors found that the $\pi-\pi$ stacking led to a strong anti-ferromagnetic interaction between spin carriers [10–12]. The $\pi-\pi$ stacking interaction should be a key factor in magnetic coupling properties, but compared with papers of bond exchange, papers of $\pi-\pi$ interaction systems remain limited [10–14] dealing with radicals or complexes with radicals as ligands. Although magnetic coupling signs of some compounds have been explained with the McConnell I

*Corresponding author. Email: shijingmin1955@gmail.com

ISSN 0095-8972 print/ISSN 1029-0389 online
http://dx.doi.org/10.1080/00958972.2011.625019

spin-polarization mechanism [15, 16] and McConnell II charge transfer mechanism [17], there are still a few questionable points or limitations [18, 19]. Factors that dominate magnetic coupling properties are not understood clearly. Therefore, it is very important to design and synthesize complexes with $\pi-\pi$ stacking and to study their magnetic coupling, and our attention has been laid to this area [20–24].

2,9-Bis(pyridin-2-methoxyl)-1,10-phenanthroline is an ideal ligand with both strong coordination and larger conjugation planes, both of which may be used to form complexes with strong $\pi-\pi$ stacking interactions, but no complex has been reported. Interest in magnetic coupling mechanism of $\pi-\pi$ stacking systems prompted us to synthesize the title mononuclear Cu(II) complex, and here we report its synthesis, crystal structure and magnetic coupling mechanism with both experimental fitting and theoretical calculations.

2. Experimental

2.1. *Materials*

2,9-Bis(pyridin-2-methoxyl)-1,10-phenanthroline was synthesized through reaction of 2,9-dichloro-1,10-phenanthroline [25] and 2-methoxylpyridine. The detailed process is as follows: 2,9-dichloro-1,10-phenanthroline (2.49 g) was dissolved into 2-methanolpyridine (20 mL), and then potassium hydroxide (2.5 g) was added into the solution and the solution was stirred for 72 h at 110°C. The yellowish sediment, after the iced water (60 mL) was added into the reaction mixture, was washed with distilled water until the eluent was neutral, and 3.0 g 2,9-bis(pyridin-2-methoxyl)-1,10-phenanthroline was obtained after drying. All other chemicals were of analytical grade and used without further purification.

2.2. *Preparation of [Cu(PMP)Br]ClO_4*

Methanol solution (10 mL) of 2,9-bis(pyridin-2-methoxyl)-1,10-phenanthroline (0.0463 g, 1.27×10^{-4} mol) was added into 5 mL water solution containing $Cu(ClO_4)_2 \cdot 6H_2O$ (0.0532 g, 1.44×10^{-4} mol), and 5 mL NaBr (0.0209 g, 2.05×10^{-4} mol) water solution was added into the solution, and then it was stirred for a few minutes. Blue single crystals (yield: 0.053 g, 65% based on 2,9-bis(pyridin-2-methoxyl)-1,10-phenanthroline) were obtained after the filtrate was allowed to slowly evaporate at room temperature for about two weeks. Elemental Anal. Calcd for $C_{24}H_{18}BrClCuN_4O_6$: (fw 637.32) C, 45.23; H, 2.85; N, 8.79; Cu, 9.97. Found (%): C, 45.46; H, 3.16; N, 9.18; Cu, 10.51.

2.3. *Physical measurements*

Infrared spectra were recorded with a Bruker Tensor 27 infrared spectrometer from 4000 to 500 cm^{-1} using KBr discs. C, H, and N elemental analyses were carried out on a Perkin-Elmer 240 instrument. Variable-temperature magnetic susceptibilities of microcrystalline powder samples were measured in a magnetic field of 1 KOe from 2 to 300 K

on a SQUID magnetometer. The data were corrected for magnetization of the sample holder and for the diamagnetic contributions of the complex ($-3.24 \times 10^{-4}\,cm^3\,mol^{-1}$), estimated from Pascal's constants.

2.4. *Computational details*

Magnetic interactions between Cu(II) ions were studied by density functional theory (DFT) coupling with the broken-symmetry (BS) approach [26–28]. The exchange coupling constant J has been evaluated by calculating the energy difference between the high-spin state (E_{HS}) and the BS state (E_{BS}). Assuming the spin Hamiltonian is defined as

$$\hat{H} = -2J\hat{S}_1 \cdot \hat{S}_2, \tag{1}$$

if the spin projected approach is used, the equation proposed by Noodleman [26–28] to extract the J value for a binuclear transition-metal complex is thus:

$$J = \frac{E_{BS} - E_{HS}}{4S_1S_2}. \tag{2}$$

To obtain exchange coupling constant J, Orca 2.8.0 calculations [29] were performed with the popular spin-unrestricted hybrid functional B3LYP proposed by Becke [30, 31] and Lee *et al*. [32], which can provide J values in agreement with the experimental data for transition-metal complexes [33, 34]. Tri-ζ basis sets with one polarization function def2-TZVP [35, 36] basis set proposed by Ahlrichs and co-workers for all atoms were used in our calculations. Strong convergence criteria were used to ensure that the results are well-converged with respect to technical parameters (the system energy was set to be smaller than 10^{-7} Hartree).

2.5. *X-ray crystallographic analysis of the complex*

A green single crystal of dimensions $0.29 \times 0.18 \times 0.15\,mm^3$ was selected and glued to the tip of a glass fiber. The determination of the crystal structure at 25°C was carried out on an X-ray diffractometer (Bruker Smart-1000 CCD) using graphite monochromated Mo-Kα radiation ($\lambda = 0.71073$ Å). Corrections for L_p factors were applied and all non-hydrogen atoms were refined with anisotropic thermal parameters. Hydrogen atoms were placed in calculated positions and refined as riding. The programs for structure solution and refinement were SHELXS-97 and SHELXL-97, respectively. The pertinent crystallographic data and structural refinement parameters are presented in table 1.

3. Results and discussion

3.1. *General characterization*

Elemental analysis indicates that the reaction of copper perchlorate hydrate with sodium bromide and 2,9-bis(pyridin-2-methoxyl)-1,10-phenanthroline yielded

Table 1. Crystal data and structure refinement for the complex.

Empirical formula	$C_{24}H_{18}BrClCuN_4$
Formula weight	637.32
Temperature (K)	298
Crystal system	Triclinic
Space group	$P\bar{1}$
Unit cell dimensions (Å, °)	
a	8.8269(14)
b	8.8322(14)
c	16.305(3)
α	79.240(2)
β	81.038(2)
γ	72.970(2)
Volume (Å^3), Z	1187.1(3), 2
Calculated density (g·cm^{-1})	1.783
Absorption coefficient (mm^{-1})	2.766
Reflections collected	6397
Unique reflections/R_{int}	4423/0.017
R_1 [$I > 2\sigma(I)$]	0.0458
wR_2 (all data)	0.1296
Goodness-of-fit on F^2	1.064
$(\Delta\rho)_{max}$ (eÅ^{-3})	0.920
$(\Delta\rho)_{min}$ (eÅ^{-3})	−0.597

[Cu(PMP)Br]ClO_4. The complex is not soluble in water, acetonitrile, acetone, dichloromethane, trichloromethane, and ethanol, is slightly soluble in methanol, and is easily soluble in dimethyl formamide. Infrared absorptions of the crystal at 1606(s) cm^{-1}, 1562(m) cm^{-1}, 1513(m) cm^{-1}, 1497(s) cm^{-1}, 1477(s) cm^{-1}, 1342(s) cm^{-1}, and 1303(s) cm^{-1} are attributed to vibrations of C=C and C=N bonds of pyridyl and 1,10-phenanthroline rings, whereas the intense peak at 1090(s) cm^{-1} is from uncoordinated perchlorate.

3.2. *Crystal structure of [Cu(PMP)Br]ClO_4*

Figure 1 shows the coordination and atom-numbering scheme. Table 2 shows coordination bond lengths from 2.009(3) Å to 2.5468(8) Å and associated angles from 80.09(12)° to 178.03(13)°. Cu1 assumes a distorted trigonal bipyramidal geometry due to its Addison constant [37] $\tau = (\beta - \alpha)/60 = 0.74$. Non-hydrogen atoms of 1,10-phenanthroline define a plane, within 0.0553 Å with a maximum deviation of −0.0918(30) for N1. In the crystal, there are three types of $\pi-\pi$ stacking [38] among adjacent complexes as shown in figure 2 (pi-1), figure 3 (pi-2), and figure 4 (pi-3), involving symmetrically related 1,10-phenanthroline rings slipped π-stacking with the relevant distances (3.7 Å as a $\pi-\pi$ stacking maximum distance [38]) being C14···C16A (or C16···C14A), 3.692(7) Å (symmetry code: $1-x$, $-y$, $1-z$) for pi-1; C1···C8A (or C1A···C8), 3.513(7) Å; C11···C11A, 3.443(6) Å (symmetry code: $-x$, $1-y$, $1-z$) for pi-2 and C11···C16A (or C11A···C16), 3.612(7) Å; C10···C13A (or C10A···C13), 3.636(6) Å; C1···C18A (or C1A···C18), 3.510(6) Å; C11···C17A (or C11A···C17), 3.633(7) Å; C10···N2A (or C10A···N2), 3.660(5) Å (symmetry code: $1-x$, $1-y$, $1-z$) for pi-3. In addition, the separation distances of Cu1···Cu1A in pi-1, pi-2, and pi-3 are 9.2634(14) Å, 8.9200(13) Å, and 7.5670(14) Å, respectively.

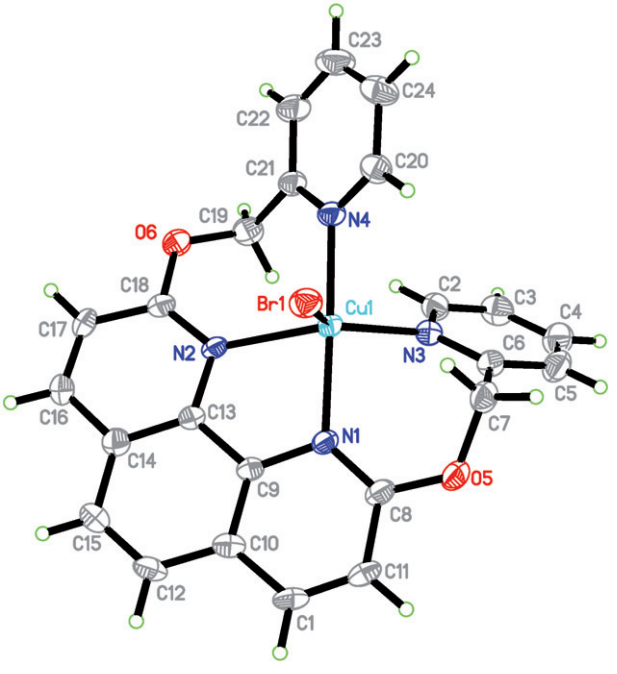

Figure 1. Coordination diagram of the title complex with the atom-numbering scheme.

Table 2. Selected bond lengths (Å) and angles (°) for the complex.

Cu1–N4	2.009(3)	Cu1–N3	2.054(3)	Cu1–N1	2.062(3)
Cu1–N2	2.171(3)	Cu1–Br	2.5468(8)		
N4–Cu1–N3	88.25(13)	N4–Cu1–N1	178.03(13)	N3–Cu1–N1	93.71(13)
N4–Cu1–N2	98.73(13)	N3–Cu1–N2	133.38(13)	N1–Cu1–N2	80.09(12)
N4–Cu1–Br1	91.01(10)	N3–Cu1–Br1	128.63(10)	N1–Cu1–Br1	87.59(9)
N2–Cu1–Br1	97.47(9)				

3.3. *Magnetic studies*

3.3.1. Experimental data. The experimental data of the variable-temperature (2−300 K) magnetic susceptibilities are shown in figure 5, where χ_M is the molar magnetic susceptibility per mononuclear Cu(II) unit and μ_{eff} is the magnetic moment per mononuclear Cu(II). Figure 5 displays increasing χ_M with decreasing temperature, until 2.00 K. The μ_{eff} value at 300 K is 1.98 B.M., large for isolated mononuclear Cu(II) (1.73 B.M. for $g_{av} = 2$) at room temperature, and the μ_{eff} value decreases slowly with temperature, reaching 1.82 B.M. at 2.0 K, suggesting weak anti-ferromagnetic coupling between adjacent Cu(II) ions. The fitting for the experimental data with Curie–Weiss formula as shown in figure 6 gave the Weiss constant $\theta = -2.99$ K $= -2.08\,cm^{-1}$, which further reveals the weak anti-ferromagnetic interaction among adjacent Cu(II) ions [39].

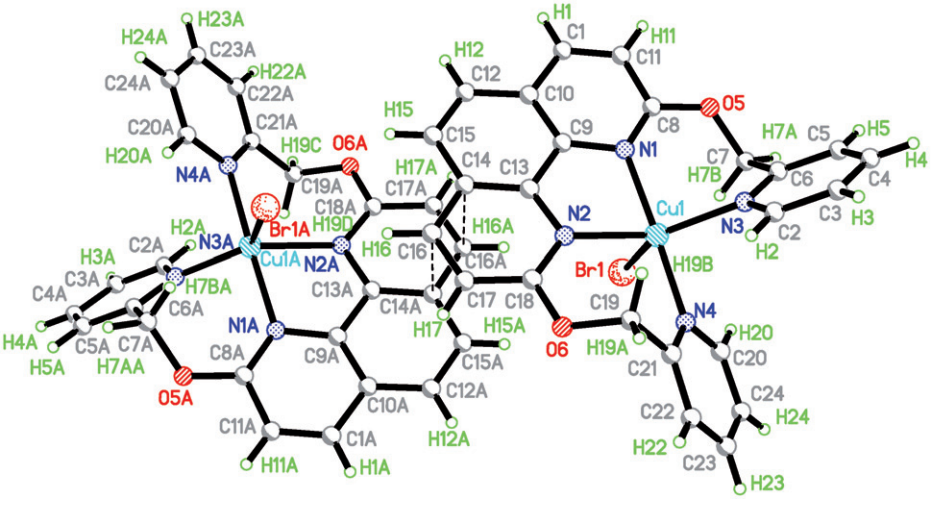

Figure 2. pi-1 $\pi-\pi$ stacking between adjacent complexes (symmetry code: $1-x, -y, 1-z$) in Model 1.

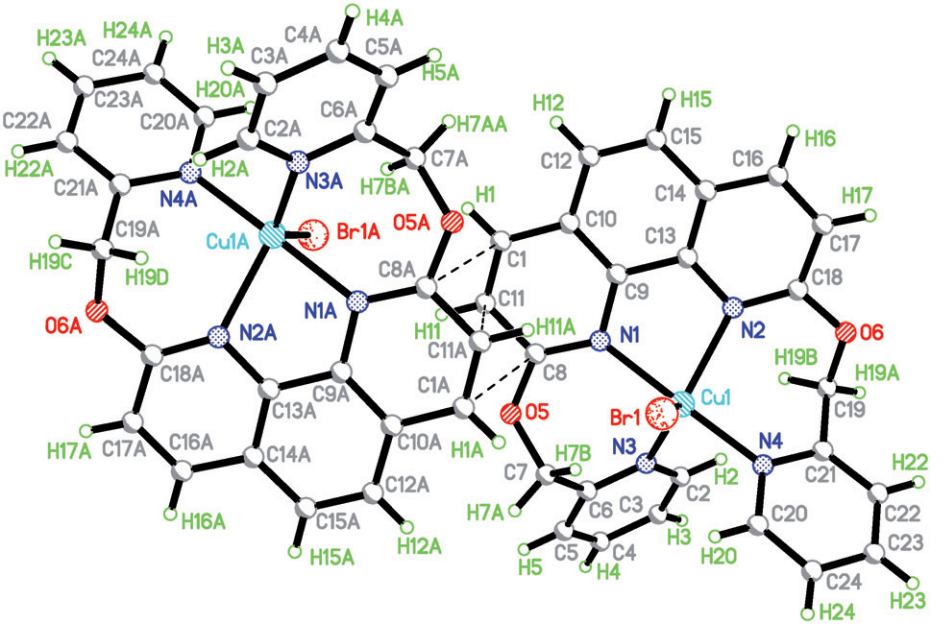

Figure 3. pi-2 $\pi-\pi$ stacking between adjacent complexes (symmetry code: $-x, 1-y, 1-z$) in Model 2.

Because there are three types of $\pi-\pi$ stacking among the adjacent complexes as mentioned above, it is very interesting to perform relevant theoretical calculations in order to understand the coupling mechanisms of the different magnetic coupling pathways.

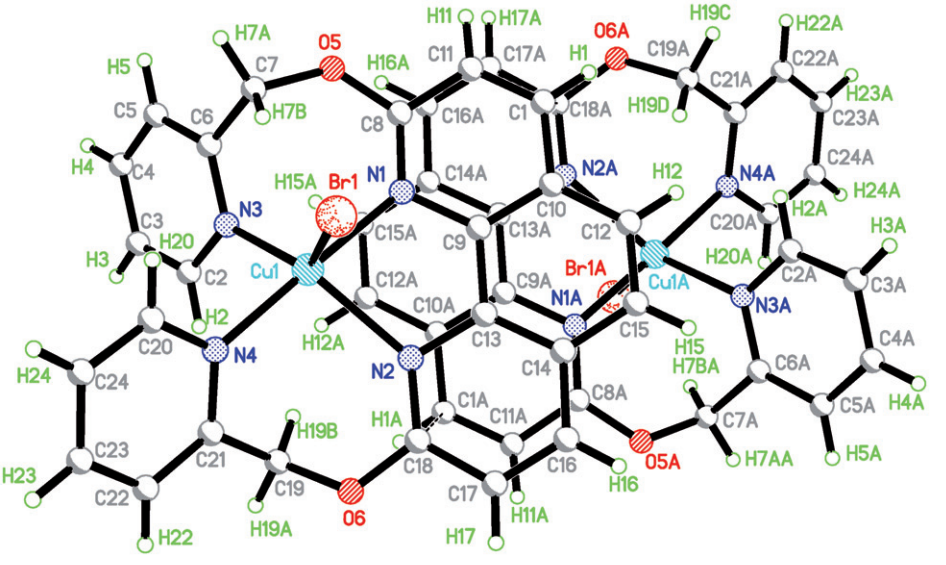

Figure 4. pi-3 $\pi-\pi$ stacking between adjacent complexes (symmetry code: A: $1-x$, $1-y$, $1-z$) in Model 3.

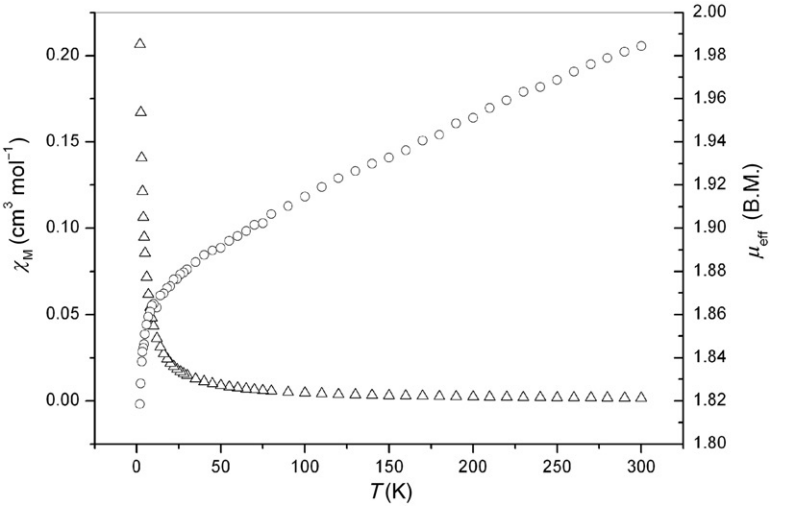

Figure 5. Plots of χ_M ($\triangle$ – the experimental data) and μ_{eff} ($^\circ$ – the experimental data) *vs.* T for the present complex.

3.3.2. Theoretical study on magnetic interaction. Density function calculations were based on Models 1, 2, and 3 as shown in figure 2, figure 3, and figure 4, respectively, representing the three types of $\pi-\pi$ stacking pi-1, pi-2, and pi-3. The calculations were constrained by data of bond lengths, associated angles, and the relevant locations of the adjacent $\pi-\pi$ stacking complexes from the X-ray structure. According to equation (2), the calculations gave $2J = 4.28\,\text{cm}^{-1}$ for Model 1 $\pi-\pi$ stacking binuclear Cu(II)

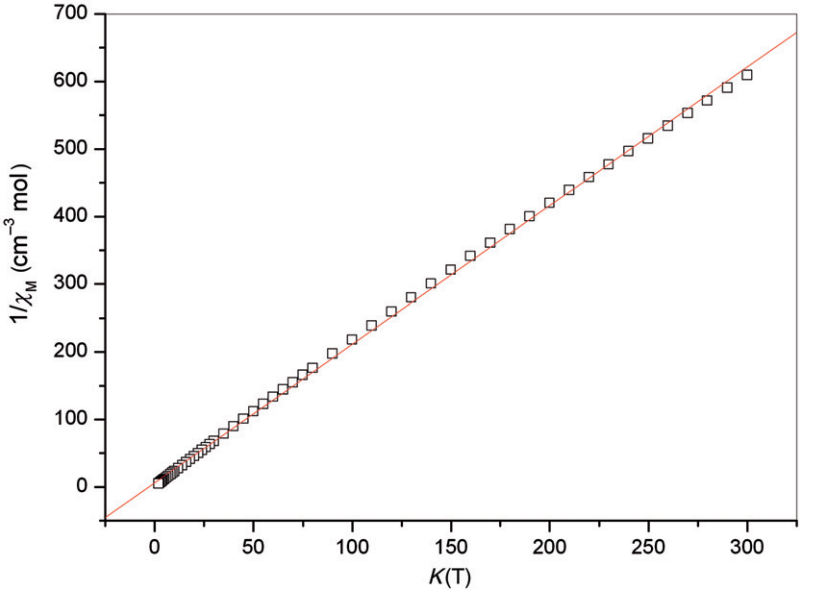

Figure 6. Thermal variation of the reciprocal susceptibility (□ – experimental data).

complex, $2J = -12.40\,cm^{-1}$ for Model 2 $\pi-\pi$ stacking binuclear Cu(II) complex, and $2J = -9.74\,cm^{-1}$ for Model 3 $\pi-\pi$ stacking binuclear Cu(II) complex; pi-1 exchange pathway functions as a weak ferromagnetic interaction, whereas both pi-2 and pi-3 exchange pathways are weak anti-ferromagnetic interactions. The calculations imply that the overall magnetic coupling behavior among the complexes should be a weak anti-ferromagnetic interaction due to the anti-ferromagnetic coupling magnitude being larger than the ferromagnetic coupling magnitude, consistent with the experimental result. In addition, the fact that the magnetic coupling magnitude of Model 2 is larger than that of Model 3 also implies that the magnetic couplings are not from dipole–dipole interaction due to the separation distance of Cu1 $\cdots$ Cu1A in Model 2 being larger than that of Model 3.

On $\pi-\pi$ stacking magnetic coupling, the sign of the McConnell I spin-polarization mechanism [15, 16] has been used to explain the ferromagnetic interaction of $[Mn(Cp^*)2]^+[Ni(dmit)2]^-$ [40], and McConnell I spin-polarization mechanism considers that a global ferromagnetic coupling arises from interaction between spin densities of opposite sign, whereas an anti-ferromagnetic coupling results from dominant interaction between spin densities of the same sign. Table 3 and figure 7 display the spin density population of the ground state of Model 1, and from table 3 the absolute value of the spin density population of each Cu(II) is smaller than 1 and the coordinated N and Br exhibit the same sign as Cu(II), suggesting that spin delocalization from the two Cu(II) 3d orbitals occurs to the coordinated atoms, whereas minus densities on a few carbon and oxygen atoms means there also exist spin-polarization phenomena in this system. Both the spin delocalization and the spin polarization benefit the magnetic coupling through the $\pi-\pi$ stacking pathway. In $\pi-\pi$ stacking two pairs of carbon atoms (C14(α) $\cdots$ C16A(β); C16(β) $\cdots$ C14A(α)) display different spin density interactions, in accord with McConnell I spin-polarization mechanism.

Table 3. Calculated atomic spin population of the ground state for Model 1.

Br1	0.124521	Br1A	0.124510
C1	−0.003146	C1A	−0.003160
C3	0.004805	C3A	0.004803
C4	−0.004341	C4A	−0.004337
C5	0.004679	C5A	0.004667
C6	−0.004086	C6A	−0.004075
C7	0.003631	C7A	0.003633
C8	−0.005991	C8A	−0.006004
C9	−0.004517	C9A	−0.004470
C10	0.004535	C10A	0.004503
C11	0.005843	C11A	0.005867
C12	0.000200	C12A	0.000274
C13	0.003233	C13A	0.003137
C14	0.000675	C14A	0.000717
C15	0.000647	C15A	0.000583
C16	−0.002231	C16A	−0.002214
C17	0.001430	C17A	0.001435
C18	−0.002975	C18A	−0.002978
C19	0.002585	C19A	0.002590
C20	−0.008852	C20A	−0.008850
C21	−0.005189	C21A	−0.005194
C22	0.007368	C22A	0.007365
C23	−0.006299	C23A	−0.006293
C24	0.007868	C24A	0.007869
Cu1	0.579396	Cu1A	0.579390
N1	0.097660	N1A	0.097645
N2	0.022761	N2A	0.022787
N3	0.066696	N3A	0.066696
N4	0.110409	N4A	0.110424
O5	−0.000559	O5A	−0.000560
O6	−0.000037	O6A	−0.000039

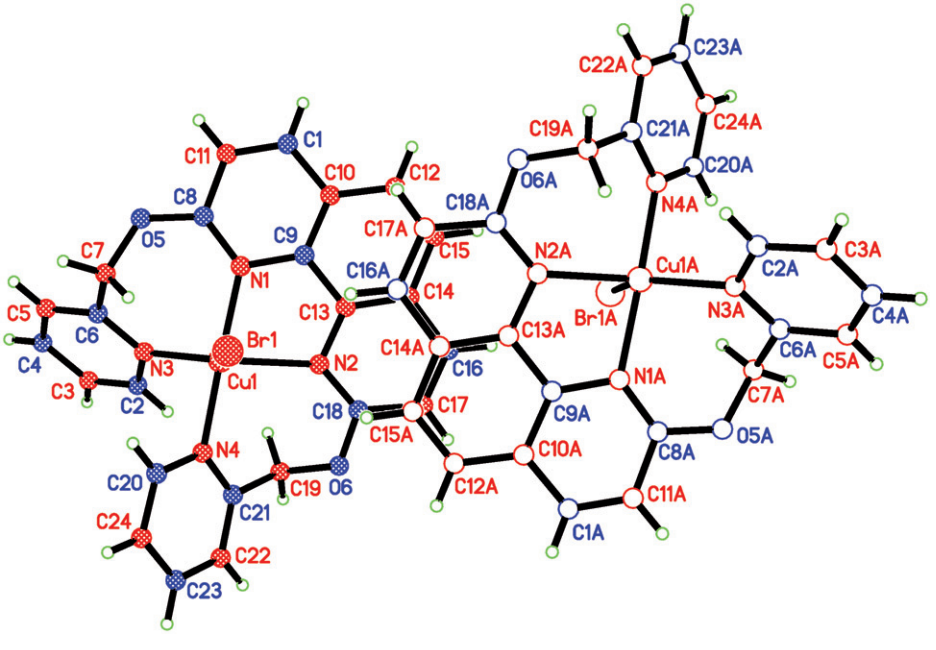

Figure 7. Calculated spin density population for Model 1; red – atoms with positive spin density and blue – atoms with negative spin density.

Table 4. Calculated atomic spin population of the ground state for Model 2.

Br1	0.128196	Br1A	−0.128195
C1	−0.002401	C1A	0.002413
C2	−0.004670	C2A	0.004671
C3	0.004115	C3A	−0.004115
C4	−0.003723	C4A	0.003722
C5	0.004034	C5A	−0.004033
C6	−0.003539	C6A	0.003555
C7	0.003719	C7A	−0.003745
C8	−0.005186	C8A	0.005191
C9	−0.003174	C9A	0.003142
C10	0.004273	C10A	−0.004362
C11	0.004880	C11A	−0.004913
C12	0.000379	C12a	−0.000336
C13	0.002708	C13A	−0.002703
C14	0.000065	C14A	−0.000140
C15	0.000264	C15A	−0.000250
C16	−0.001600	C16A	0.001586
C17	0.001308	C17A	−0.001311
C18	−0.002810	C18A	0.002816
C19	0.002379	C19A	−0.002380
C20	−0.008104	C20A	0.008106
C21	−0.004181	C21A	0.004189
C22	0.006821	C22A	−0.006824
C23	−0.005559	C23A	0.005560
C24	0.007165	C24A	−0.007167
Cu1	0.577504	Cu1A	−0.577490
N1	0.095495	N1A	−0.095446
N2	0.022555	N2A	−0.022537
N3	0.063160	N3A	−0.063171
N4	0.110984	N4A	−0.111003
O5	−0.000407	O5A	0.000406
O6	0.000020	O6A	−0.000021

Table 4 and figure 8 reveal the spin density population of the ground state of Model 2. Similar to Model 1 the spin delocalization also occurs in Model 2 from Cu(II) to the associated coordinated atoms, and there also exists spin polarization in Model 2. In the $\pi-\pi$ stacking system, three pairs of carbons (C1(β)$\cdots$C8A(α), C8(β)$\cdots$C1A(α), and C11(α)$\cdots$C11A(β)) exhibit different spin density interactions, which is clearly unable to be explained with McConnell I spin-polarization mechanism and the same example is reported in a Cu(II) complex [24].

The spin density population of the ground state of Model 3 is exhibited in table 5 and figure 9, and just like Model 1 and Model 2 there are both spin delocalization and spin polarization in this system. In the $\pi-\pi$ stacking there are two pairs of carbons (C11(α)$\cdots$C16A(α); C16(β)$\cdots$C11A(β)) that exhibit the same spin density interaction and eight pairs (C10(α)$\cdots$C13A(β); C13(α)$\cdots$C10A(β); C1(β)$\cdots$C18A(α); C18(β)$\cdots$C1A(α); C11(α)$\cdots$C17A(β); C17(α)$\cdots$C11A(β); C10(α)$\cdots$N2A(β); N2(α)$\cdots$C10A(β)) display different spin density interactions; the number of the different spin density interactions is larger than that of the same spin density interaction, and, mostly, neither the shortest distance nor the largest spin density are found on the pairs of atoms with the same spin density. Just like in Model 2 the McConnell I spin-polarization mechanism is unable to explain the anti-ferromagnetic

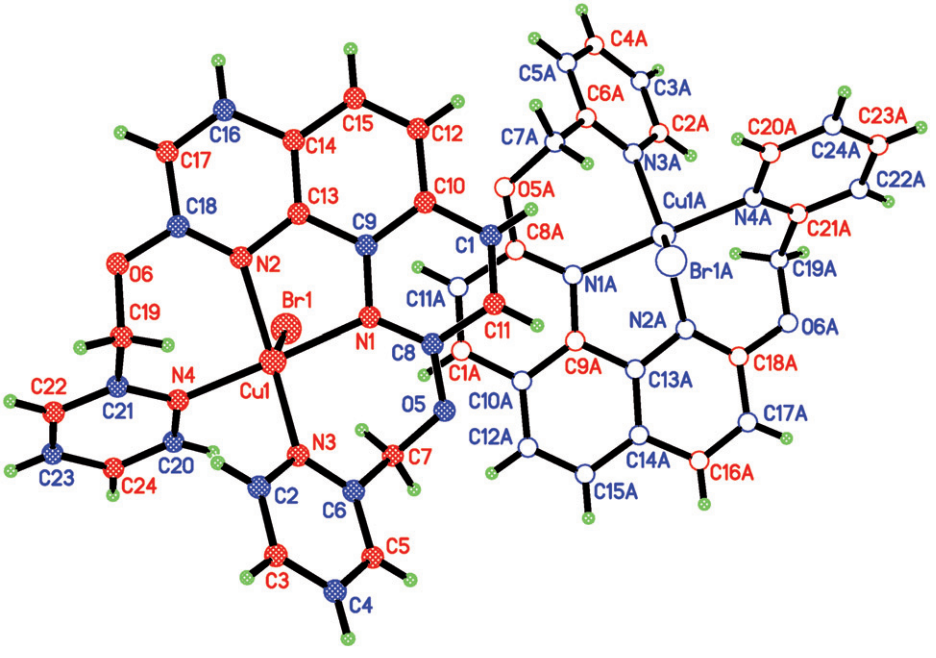

Figure 8. Calculated spin density population for Model 2; red – atoms with positive spin density and blue – atoms with negative spin density.

Table 5. Calculated atomic spin population of the ground state for the Model 3.

Br1	0.171683	Br1A	−0.171685
C1	−0.002164	C1A	0.002080
C2	−0.003499	C2A	0.003514
C3	0.003488	C3A	−0.003502
C4	−0.003367	C4A	0.003371
C5	0.003623	C5A	−0.003620
C6	−0.003154	C6A	0.003137
C7	0.002987	C7A	−0.002973
C8	−0.004697	C8A	0.004689
C9	−0.002245	C9A	0.002186
C10	0.003638	C10A	−0.003498
C11	0.004858	C11A	−0.004813
C12	0.000954	C12A	−0.00098
C13	0.002151	C13A	−0.002044
C14	0.000410	C14A	−0.000559
C15	0.000057	C15A	0.000009
C16	−0.001876	C16A	0.001971
C17	0.001291	C17A	−0.001338
C19	0.001367	C19A	−0.00137
C20	−0.007940	C20A	0.007934
C21	−0.003240	C21A	0.003227
C22	0.006654	C22A	−0.006632
C23	−0.005401	C23A	0.005386
C24	0.006875	C24A	−0.006868
Cu1	0.556924	Cu1A	−0.556913
N1	0.087377	N1A	−0.087348
N2	0.017391	N2A	−0.017432
N3	0.056334	N3A	−0.056337
N4	0.109671	N4A	−0.109685
O1	−0.000257	O1A	0.000261
O2	−0.000295	O2A	0.000291

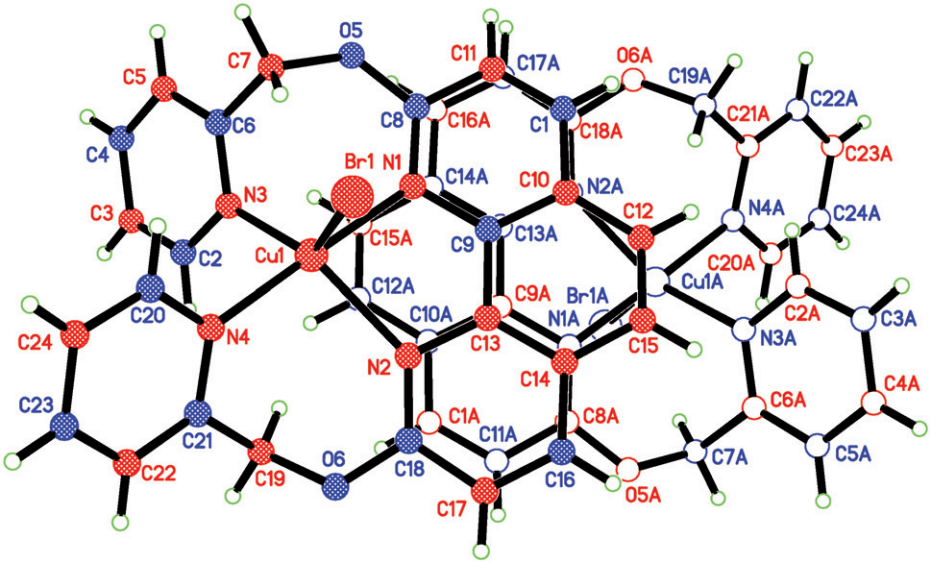

Figure 9. Calculated spin density population for Model 3; red – atoms with positive spin density and blue – atoms with negative spin density.

coupling mechanism of Model 3. Obviously, the present magnetic coupling phenomena are a challenge to explain.

4. Conclusion

A mononuclear Cu(II) complex with 2,9-bis(pyridin-2-methoxyl)-1,10-phenanthroline and bromide as terminal ligands has been synthesized; its crystal displays three types of $\pi-\pi$ stacking magnetic coupling pathways. The fitting on its variable-temperature magnetic susceptibilities with Curie–Weiss formula reveals that there exists weaker anti-ferromagnetic coupling among adjacent Cu(II) ions. Theoretical calculations reveal that one magnetic coupling pathway exhibits weak ferromagnetic coupling and the other two magnetic coupling pathways display weak anti-ferromagnetic couplings; the overall anti-ferromagnetic coupling magnitude is larger than that of the ferromagnetic coupling. The magnetic coupling sign of the ferromagnetic coupling accords with McConnell I spin polarization, whereas the anti-ferromagnetic coupling signs are not explained with McConnell I spin polarization. Explaining the magnetic coupling sign remains a challenge.

Supplementary material

CCDC 800542 contains detailed information of the crystallographic data for this article, and these data can be obtained free of charge from the Cambridge Crystallographic Data Centre *via* http://www.ccdc.cam.ac.uk/data_request/cif.

Acknowledgments

This work was supported by the National Natural Science Foundation of China (Grant No. 20971080) and the Natural Science Foundation of Shandong Province (Grant Nos ZR2009BM026 and ZR2009BL002).

References

[1] J.R. Friedman, M.P. Sarachik, J. Tejada, R. Ziolo. *Phys. Rev. Lett.*, **76**, 3830 (1996).
[2] G.L.J.A. Rickken, E. Raupack. *Nature*, **405**, 932 (2000).
[3] S. Tanase, J. Reedijk. *Coord. Chem. Rev.*, **250**, 2501 (2006).
[4] H. Li, T.-T. Sun, S.-G. Zhang, J.-M. Shi. *J. Coord. Chem.*, **63**, 1531 (2010).
[5] C. Wang, J. Li, Y.-W. Ren, F.-G. He, G. Meke, F.-X. Zhang. *J. Coord. Chem.*, **61**, 4033 (2008).
[6] H. Li, C. Hou, J.-M. Shi, S.-G. Zhang. *J. Coord. Chem.*, **61**, 3501 (2008).
[7] J.-M. Li, X. Jin. *J. Coord. Chem.*, **62**, 2610 (2009).
[8] J.-M. Shi, Q.S. Liu, W. Shi. *J. Coord. Chem.*, **62**, 1121 (2009).
[9] L.-L. Li, K.-J. Lin, C.-J. Ho, C.-P. Sun, H.-D. Yang. *Chem. Commun.*, 1286 (2006).
[10] N.P. Gritsan, A.V. Lonchakov, E. Lork, R. Mews, E.A. Pritchina, A.V. Zibarev. *Eur. J. Inorg. Chem.*, 1994 (2008).
[11] K. Goto, T. Kubo, K. Yamanoto, K. Nakasuji, K. Sato, D. Shiomi, T. Takui, M. Kubota, T. Kobayashi, K. Yakusi, J. Ouyang. *J. Am. Chem. Soc.*, **121**, 1619 (1999).
[12] B.D. Koivisto, A.S. Ichimura, R. McDonald, M.T. Lemaire, L.K. Thompson, R.G. Hicks. *J. Am. Chem. Soc.*, **128**, 690 (2006).
[13] L. Norel, F. Pointillart, C. Train, L.-M. Chamoreau, K. Boubekeur, Y. Journaux, A. Brieger, D.J.R. Brook. *Inorg. Chem.*, **47**, 2396 (2008).
[14] X.M. Ren, S. Nishihara, T. Akutagawa, S. Noro, T. Nakamura. *Inorg. Chem.*, **45**, 2229 (2006).
[15] H.M. McConnell. *J. Chem. Phys.*, **39**, 1910 (1963).
[16] K. Yoshizawa, R. Hoffmann. *J. Am. Chem. Soc.*, **117**, 6921 (1995).
[17] J.S. Miller, A.J. Epstein. *J. Am. Chem. Soc.*, **109**, 3850 (1987).
[18] M. Deumal, J.J. Novoa, M.J. Bearpark, P. Celani, M. Olivacci, M.A. Robb. *J. Phys. Chem. A*, **102**, 8404 (1998).
[19] M. Deumal, J. Cirujeda, J. Veciana, J.J. Novoa. *Chem. Eur. J.*, **5**, 1631 (1995).
[20] H. Li, S.-G. Zhang, L.M. Xie, L. Yu, J.-M. Shi. *J. Coord. Chem.*, **64**, 1456 (2011).
[21] J.-M. Shi, X.-Z. Meng, Y.-M. Sun, H.-Y. Xu, W. Shi, P. Cheng, L.-D. Liu. *J. Mol. Struct.*, **917**, 164 (2009).
[22] L. Yu, J.-M. Shi, Y.-Q. Zhang, Y.-Q. Wang, Y.-N. Fan, G.-Q. Zhang, W. Shi, P. Cheng. *J. Mol. Struct.*, **987**, 138 (2011).
[23] C. Hou, J.-M. Shi, Y.-M. Sun, W. Shi, P. Cheng, L.-D. Liu. *Dalton Trans.*, **37**, 5970 (2008).
[24] Y.-H. Chi, L. Yu, J.-M. Shi, Y.-Q. Zhang, T.Q. Hu, G.Q. Zhang, W. Shi, P. Cheng. *Dalton Trans.*, **40**, 1453 (2011).
[25] J. Lewis, T.D. O'Donghue. *J. Chem. Soc., Dalton Trans.*, 736 (1980).
[26] L. Noodleman. *J. Chem. Phys.*, **74**, 5737 (1981).
[27] L. Noodleman, E.J. Baerends. *J. Am. Chem. Soc.*, **106**, 2316 (1984).
[28] L. Noodleman, D.A. Case. *Adv. Inorg. Chem.*, **38**, 423 (1992).
[29] F. Neese. *An Ab Initio, DFT and Semiempirical Electronic Structure Package, Program Version 2.7, Revision 0*, Lehrstuhl fuer Theoretische Chemie Institut fuer Physikalische und Theoretische Chemie, Universitaet Bonn, Germany, (2010).
[30] A.D. Becke. *J. Chem. Phys.*, **98**, 5648 (1993).
[31] A.D. Becke. *Phys. Rev. A*, **38**, 3098 (1988).
[32] C. Lee, W. Yang, R.G. Parr. *Phys. Rev. B*, **37**, 785 (1988).
[33] J. Cano, E. Ruiz, S. Alvarez, M. Verdaguer. *Comments Inorg. Chem.*, **20**, 27 (1998).
[34] E. Ruiz, P. Alemany, S. Alvarez, J. Cano. *J. Am. Chem. Soc.*, **119**, 1297 (1997).
[35] A. Schaefer, H. Horn, R. Ahlrichs. *J. Chem. Phys.*, **97**, 2571 (1992).
[36] F. Weigend, R. Ahlrichs. *Phys. Chem. Chem. Phys.*, **7**, 3297 (2005).

[37] A.W. Addison, T.N. Rao, J. Reedjik, J. van Rijn, C.G. Verschoor. *J. Chem. Soc., Dalton Trans*., 1349 (1984).
[38] C. Janiak. *J. Chem. Soc., Dalton Trans*., 3885 (2000).
[39] M.V. Fedin, S.L. Veber, K.Y. Maryunina, G.V. Romanenko, E.A. Suturinu, N.P. Gritsan, R.Z. Sagdeev, V.I. Ovcharenko, E.G. Bagryanskaya. *J. Am. Chem. Soc*., **132**, 13886 (2010).
[40] C. Faulmann, E. Rivière, S. Dorbes, F. Senocq, E. Coronado, P. Cassoux. *Eur. J. Inorg. Chem*., 2880 (2003).